

1 **An optical study of the combustion and flame development of ammonia-diesel**  
2 **dual-fuel engine based on flame chemiluminescence**

3

4 Wanchen Sun <sup>a</sup>, Wenpeng Zeng <sup>a</sup>, Liang Guo <sup>a</sup>, Hao Zhang <sup>a\*</sup>, Yuying Yan <sup>b</sup>, Shaodian Lin <sup>a</sup>, Genan  
5 Zhu <sup>a</sup>, Mengqi Jiang <sup>a</sup>, Changyou Yu <sup>a</sup>, Fei Wu <sup>a</sup>

6 <sup>a</sup> *State Key Laboratory of Automotive Simulation and Control, Jilin University, Changchun 130025,*  
7 *China*

8 <sup>b</sup> *Faculty of Engineering, the University of Nottingham, Nottingham, UK, NG7 2RD*

9

10 **Abstract**

11 Under the background of the "carbon peak and carbon neutrality", the development and  
12 utilization of zero-carbon fuels, represented by green ammonia and green hydrogen, has gained  
13 attention from all walks of life. Among them, the problems of transportation and storage of hydrogen  
14 restrict its industrial development, while ammonia has significant advantages as a suitable hydrogen  
15 energy carrier for the power systems. The ammonia-diesel dual-fuel engine enables the mixture to  
16 be stratified in a time-activated multi-point ignition mode to promote efficient and clean combustion  
17 of ammonia. To investigate the combustion and flame development of the ammonia-diesel dual-fuel  
18 engine, an optical diagnostic study was carried out on a self-refit dual-fuel optical engine. The results

---

\* Corresponding author, Address for correspondence: State Key Laboratory of Automotive Simulation and Control, Jilin University, Changchun 130025, People's Republic of China.

*E-mail address:* haozhang@jlu.edu.cn (Hao Zhang).

19 show that the combustion inertia and lower flame temperature of ammonia can inhibit combustion  
20 and lead to lower cyclic heat release in the ammonia-diesel dual-fuel combustion (ADDC) mode,  
21 which in turn reduces the indicated mean effective pressure (IMEP). Different from the yellow-  
22 white flame produced by the high-temperature soot radiation in pure diesel combustion (PDC) mode,  
23 the flame in the ADDC mode appears orange. The peak of flame area (FR) percentage and flame  
24 natural luminosity (FNL) of the 80% ammonia ratio ADDC mode decrease by 60% and 92%,  
25 respectively, compared to the peaks at PDC mode. The ammonia combustion flame is mainly  
26 concentrated around the diesel flame, and at the same time achieves good ignition performance at  
27 all ammonia ratios. In contrast to the PDC mode where the FR and FNL decrease rapidly as the  
28 diesel injection timing (DIT) advances, the flame pattern of the ADDC mode does not respond  
29 significantly to the DIT.

30

31 *Keywords:* Ammonia-diesel dual-fuel combustion; Combustion characteristics; Flame  
32 development; Ammonia ratio; Diesel injection timing

33

34 **Highlights:**

- 35 ● An optical study of the ADDC mode was conducted.
- 36 ● Ammonia premixing leads to lower cyclic heat release and IMEP.
- 37 ● The ammonia flame is mainly concentrated around the diesel flame.
- 38 ● The effect of flame pattern on DIT is not significant in the ADDC mode.

39

<b>Abbreviations</b>
----------------------

ICE	Internal combustion engine	FNL	Flame natural luminosity
CI	Compression-ignition	HRR	Heat release rate
SI	Spark ignition	ATDC	After top dead center
HEI	High energy ignition	COV	Coefficient of cyclic variation
ADDC	Ammonia-diesel dual-fuel combustion	DIT	Diesel injection timing
SCR	Selective catalytic reduction	CD	Combustion duration
LIF	Laser-induced fluorescence	ID	Ignition delay
LII	Laser-induced incandescence	CA	Crank angle
PIV	Particle imaging velocimetry	CN	Cetane number
SRS	Stimulated Raman scattering	RON	Research octane number
EGR	Exhaust gas recirculation	IMEP	Indicated mean effective pressure
FR	Flame area	PDC	Pure diesel combustion

## 40 **1. Introduction**

41 In order to overcome the greenhouse effect of carbon dioxide on the global ecology,  
42 governments have put forward " carbon peak and carbon neutrality goals " in recent years <sup>[1]</sup>. In the  
43 circumstance, the transformation of the global energy structure has received widespread attention,  
44 and zero-carbon renewable energy, represented by wind energy, solar energy, and ocean energy, has  
45 been rapidly developed <sup>[2-4]</sup>. However, renewable energy sources are subject to significant  
46 fluctuations due to weather, time, geography, and season, so the development of renewable energy  
47 must be combined with the progress of energy storage technologies. Among all the energy storage,  
48 chemical energy storage is the most flexible one, which can be moved, stored, and distributed at a  
49 low cost <sup>[5, 6]</sup>. Currently, chemical energy storage, represented by carbon-neutral fuels such as green

50 hydrogen, green ammonia, biomass fuels, and green electric synthetic liquid fuels, is one of the most  
51 popular form of zero-carbon energy storage. Among them, ammonia and hydrogen have a clear  
52 application prospect in the short term due to its relatively mature technology system <sup>[7-9]</sup>.

53 At present, hydrogen, as an efficient and clean secondary zero-carbon energy, is attracting  
54 widespread attention in the application of hydrogen fuel cells and hydrogen internal combustion  
55 engines (ICEs) <sup>[10, 11]</sup>. However, hydrogen still faces a series of technical challenges in terms of  
56 production, transportation, storage, and end-use applications, and the consequent long-tail effect  
57 restricts its industrial development <sup>[12]</sup>. Ammonia (NH<sub>3</sub>) as a suitable carrier of hydrogen energy,  
58 with its complete combustion products of nitrogen and water, is also a carbon-neutral fuel. Ammonia  
59 has clear advantages over hydrogen as the powertrain fuel for several reasons <sup>[13]</sup>. Firstly, ammonia  
60 can be completely liquefied at 298.15 K and 0.9 MPa, and the hydrogen content density (106.4  
61 kg/m<sup>3</sup>) and low heat value (11.213 GJ/m<sup>3</sup>) of liquid ammonia are higher than those of liquid  
62 hydrogen (70.8 kg/m<sup>3</sup> and 9.168 GJ/m<sup>3</sup>). Secondly, the economic cost of ammonia is relatively low,  
63 with the unit energy price of ammonia (13.3 USD/GJ) being lower than that of hydrogen (35.2  
64 USD/GJ) and gasoline (29.1 USD/GJ), while the storage cost of ammonia is only 1/26th to 1/30th  
65 of that of hydrogen <sup>[14]</sup>. In addition, the technology for large-scale industrial production of ammonia  
66 is well established. The production efficiencies have been reached over 90% and the associated  
67 infrastructures have been globally arranged <sup>[15]</sup>. Finally, ammonia combustion is characterized by a  
68 slow flame speed and narrow combustion limits, which makes it less likely to cause an explosion,  
69 so it is of high security. As a result, ammonia is expected to be the ideal solution for the green  
70 transformation of future energy systems as a source of energy for thermal and power equipment <sup>[16,</sup>  
71 <sup>17]</sup>.

72 The physicochemical properties of ammonia make it suitable for use as a fuel in power systems,  
73 so it has a promising market in power generation, automobiles, ships, aircrafts, and rockets. In  
74 particular, the application of ammonia in the widely used ICEs is of strategic importance [18-20].  
75 However, ammonia is more difficult to burn in the ICEs than fossil fuels such as petrol and diesel  
76 [21]. In the early years, the US military had conducted several experiments with pure ammonia as a  
77 fuel in the compression-ignition (CI) engine, and the results showed that the compression ratio  
78 needed to be increased to 35:1 to ensure stable combustion of the pure ammonia engine. Subsequent  
79 research showed that pure ammonia can be burned in an ignition engine using the technique of  
80 variable compression ratio and multiple sparks plug ignition, but the slow flame propagation of  
81 ammonia combustion and the significant quenching effect led to unstable and inefficient combustion  
82 [22]. As a result, it is difficult to use ammonia as an ICE fuel alone and reactivity enhancer is required  
83 to improve its combustion performance [23]. Ammonia is currently used by two main ways in ICEs.  
84 In the spark ignition (SI) engine, ammonia is mixed with one or more reactive enhancer such as  
85 hydrogen and then ignited by high energy ignition (HEI) or jet ignition. In the CI engine, ammonia  
86 is used as a premixed fuel and ignited by the high reactivity fuel such as diesel [24, 25]. Among them,  
87 the ammonia-premixed ignition combustion mode enables the mixture to be stratified by flexibly  
88 adjusting the fuel injection strategy, which promotes efficient and clean combustion of ammonia by  
89 means of multi-point ignition. Thus, the ammonia-premixed ignition combustion mode is expected  
90 to be the ideal solution for the heavy-duty ammonia-fueled engines [26, 27]. In addition, ammonia is  
91 suitable for use in CI engines with high compression ratio to improve thermal efficiency due to the  
92 high octane number and excellent anti-explosion property. Also, the CI engines provide better torque  
93 characteristics and power coverage for a wider range of applications. Consequently, ammonia-

94 fueled CI engines based on ammonia-premixed ignition combustion have great potential for  
95 applications in heavy truck power, marine power, and power generation [28, 29]. Reiter et al. achieved  
96 stable operation of ammonia-diesel dual-fuel combustion (ADDC) mode in a CI engine and  
97 increased the engine combustion efficiency to over 95% at the ammonia ratios of 40-60% [30]. Niki  
98 et al. further investigated the ADDC mode and found that a multiple injection strategy could achieve  
99 thermal efficiency equivalent to that of the conventional diesel engine. However, the low flame  
100 speed, quenching, and gapping effects of ammonia led to low ammonia combustion efficiency and  
101 deteriorating emissions [31]. Sun et al. suggested that selective catalytic reduction (SCR) technology  
102 has considerable potential for reducing NO<sub>x</sub> and unburned ammonia emissions from ADDC engines  
103 [32]. Accordingly, the ADDC mode requires in-depth optimization of its combustion process to  
104 exploit the performance potential of ammonia-fueled CI engines.

105       The development of optical measurement technology has provided new means and methods  
106 for the research of ICEs [33, 34]. In contrast to traditional thermodynamic investigations, which focus  
107 on the macroscopic combustion and emission characteristics of ICEs, the optical measurements  
108 focus on the internal combustion processes of ICEs, which provide an excellent insight into the  
109 development of combustion flame and the pollutant generation mechanism under different  
110 combustion modes [35-37]. The main optical measurement techniques currently used in ICE research  
111 include flame chemiluminescence, laser-induced fluorescence (LIF), laser-induced incandescence  
112 (LII), particle imaging velocimetry (PIV) and stimulated Raman scattering (SRS), which provide a  
113 full range of diagnostics for fuel spray, mixture forming, ignition processes, combustion processes  
114 and pollutant formation in ICEs [38, 39]. Among them, the use of high-speed photography combined  
115 with flame chemiluminescence provides a deep analysis of flame development and flame

116 morphology during the combustion processes of ICEs, which is important for understanding the  
117 spatial and temporal evolution of the in-cylinder flame under different combustion modes and  
118 boundary conditions [40, 41]. Ihracska et al. studied the flame characters of a spark-ignited engine  
119 using high-speed imaging, fitting image projections of flame to circles and ellipses, followed by  
120 statistical evaluation of the flame centroid, flame perimeter, and flame shape [42]. Hult et al. arranged  
121 multiple high-speed cameras in a marine two-stroke optical engine to map the spatial position of the  
122 in-cylinder flame and reconstruct the 3D flame profile to extract characteristics such as flame length,  
123 flame height, ignition source position, and flame direction [43]. Lee et al. studied the influence of  
124 various conditions such as injection timing, exhaust gas recirculation (EGR), and swirl ratio on the  
125 flame propagation process based on an optical engine, and clarified the effect of swirl on the spray  
126 and flame morphology [44]. Therefore, an optical diagnostic study on the ADDC mode is significant  
127 for a deep understanding on many combustion details, as well as proposing combustion control  
128 strategies to improve the performance of ammonia-fueled engines.

129 This study investigates the ADDC mode in a modified single-cylinder CI optical engine using  
130 flame luminescence combined with high-speed photography. The combustion characteristics and  
131 flame development of the ADDC mode are analyzed in depth from the thermodynamic and optical  
132 perspectives respectively. The influence mechanism of the fuel injection strategy on the ADDC  
133 engine is clarified and the regulation direction of combustion boundary conditions to achieve fast  
134 and stable combustion in ammonia-fueled engines is proposed.

## 135 **2. Experimental apparatus and procedure**

### 136 *2.1 Optical engine and operating conditions*

137 The optical engine used in this study had been refitted from a single-cylinder, four-stroke, CI,

138 upright engine. The piston of the optical engine had been converted to a "Bowditch" type extended  
 139 piston. The extended piston had a transparent piston top with a lowered 45-degree reflector, forming  
 140 a light path for viewing the combustion process in the cylinder. The optical engine was dragged by  
 141 a three-phase asynchronous motor to a stable speed, and the fuel was injected in the specific cycle  
 142 to achieve skip fire. The specifications of the optical engine are shown in **Table 1**.

143 **Table 1.** The specifications of the optical engine

Category	Properties
Geometric compression ratio	13
Cylinder diameter / mm	105
Piston stroke / mm	114.3
Connecting rod length / mm	190
The number of nozzles holes	7
Engine valve lift / mm	11
Engine valve count	4

144 The support systems had also been designed and developed to form an optical test platform  
 145 together with the optical engine. The support systems included a high-pressure common-rail fuel  
 146 injection system, an ammonia injection system, an intake and exhaust system, a variable valve  
 147 system, a high-speed photography system, and a combustion analysis system. The schematic  
 148 diagram of the optical test platform is shown in **Fig. 1**. The key parameters of the high-speed camera  
 149 are shown in **Table 2**. And the more details on the platform and high-speed photography method  
 150 can be found in previous work <sup>[40]</sup>. The RGB images obtained by the high-speed photography

151 method were cropped, denoised, and enhanced. Then the treatments of Di Iorio and Zhang et al.  
 152 were referred to obtain information on the flame area (FR), flame natural luminosity (FNL), and  
 153 flame center [45 46]. Based on the above information, it is possible to explore the influence of the  
 154 combustion and flame development process on the ADDC, and to reveal the essential mechanism  
 155 of the impact on macroscopic combustion characteristics and engine performance. In addition, the  
 156 combustion analysis system is comprised of AVL GH12D pressure sensor, KISTLER 2614B  
 157 encoder, and PowerMAC CA300A8 combustion analyzer, with a sampling resolution of 0.1°C.A.  
 158 The HRR (heat release rate) was calculated based on the multivariate exponential algorithm and the  
 159 Rassweiler and Withrow model.

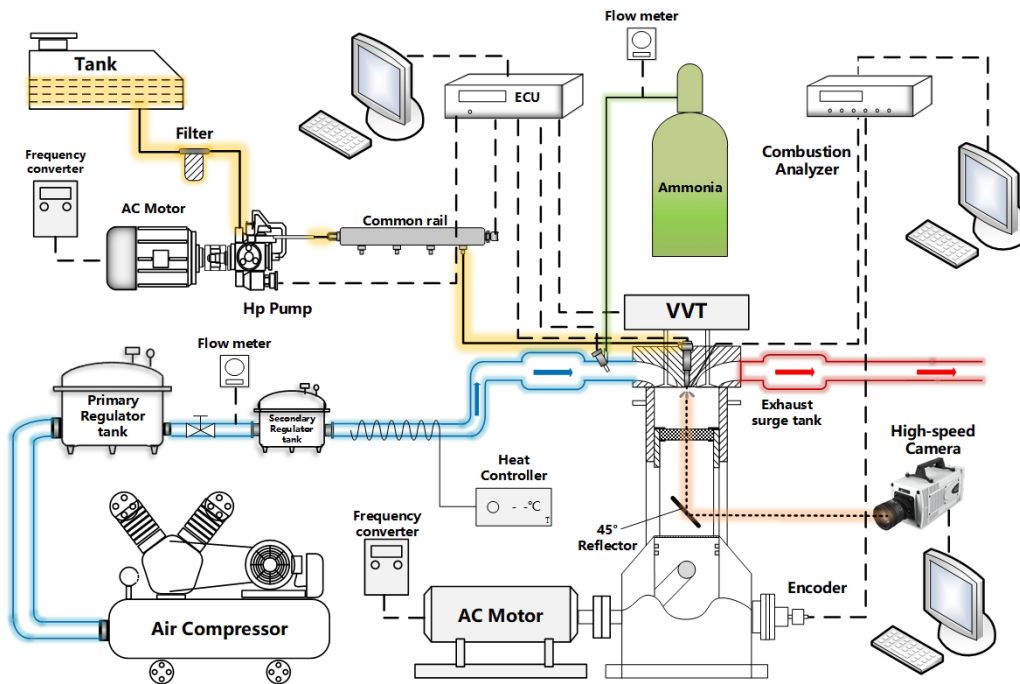


Fig. 1 The schematic diagram of the optical test platform

160

Table 2. The key parameters of the high-speed camera

Category	Parameters
Resolution	512*512

Exposure time /  $\mu$ s 30

Aperture level 7

---

161 2.2 Experimental procedure

162 In this study, the engine speed was kept at  $1000 \pm 5$  r/min, the in-cylinder injection energy was  
163 maintained at 1438 J/cycle and the common rail pressure was fixed at  $100 \pm 3$  MPa. The ammonia  
164 was delivered at  $-300^\circ\text{CA}$  after top dead center (ATDC) in the intake stroke using port injection with  
165 a pressure of 3 bar. To ensure proper combustion during the test conditions, the intake air and the  
166 cooling water were heated to  $353 \pm 2$  K and  $358 \pm 2$  K, respectively, and the intake mass was adjusted  
167 to  $60 \pm 1$  kg/h. Due to the limitations of the structural strength of the optical engine, three tests were  
168 conducted for each operating condition the data were considered valid when the coefficient of cyclic  
169 variation ( $\text{COV}_{\text{imep}}$ ) of the three tests was within 5%. Firstly, the experiment was conducted by  
170 fixing the diesel injection timing (DIT) at  $-9^\circ\text{CA}$  ATDC and investigating the effect of ammonia  
171 ratios on the ADDC mode. The heat value of ammonia was adjusted to 0%, 20%, 30%, 40%, 50%,  
172 60%, 70%, and 80% of the total heat value of the in-cylinder fuel. After that, the DIT was adjusted  
173 between  $-5^\circ\text{CA}$  ATDC and  $-13^\circ\text{CA}$  ATDC ( $2^\circ\text{CA}$  interval) at the 50% ammonia ratio (based on the  
174 heat value) to study the effect of DIT on the ADDC mode. The main physical-chemical  
175 characteristics of the ammonia and diesel used in this study are shown in **Table 3**.

176 **Table 3.** The main physical-chemical characteristics of the test fuels

---

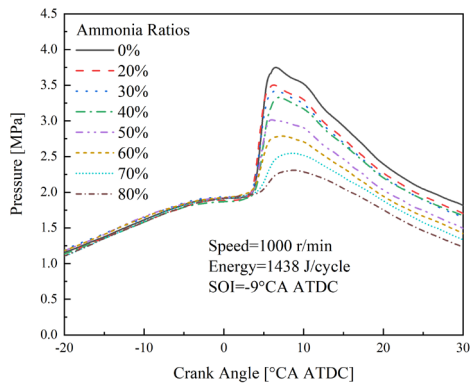
Fuel properties	Ammonia	Diesel
Hydrogen content by mass / (%)	17.7	12.6
Boiling point / ( $^\circ\text{C}$ )	-33.4	180-360

---

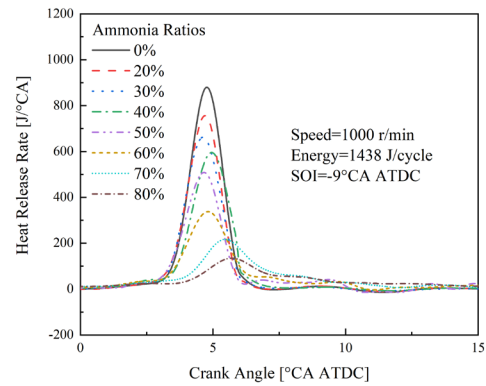
Latent heat of vaporization / (kJ·kg <sup>-1</sup> )	~	0.27
Low heat value / (MJ·kg <sup>-1</sup> )	18.6	42.69
Laminar flame speed / (m·s <sup>-1</sup> )	0.07	~
Minimum ignition energy / (MJ)	680	~
Cetane number (CN)	~	52
Research octane number (RON)	130	15-25
Theoretical air-fuel ratio	6.06	14.3

## 177 3. Results and discussions

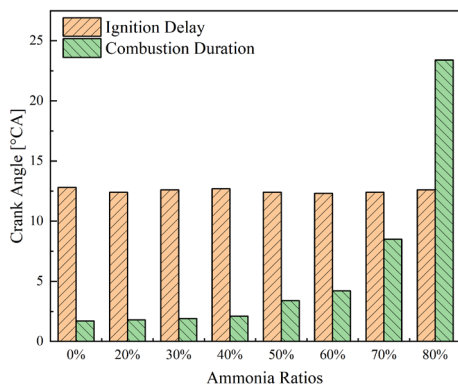
### 178 3.1 Effects of ammonia ratios on the combustion characteristics of the ADDC engine



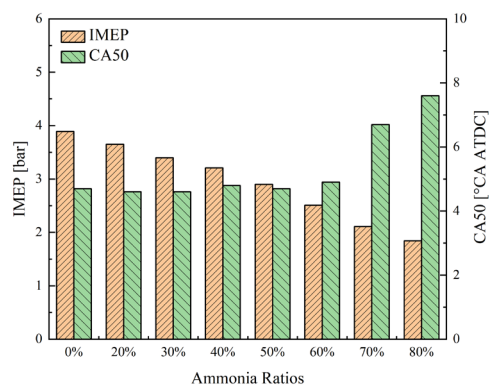
(a) Cylinder pressure



(b) HRR



(c) Ignition delay (ID) and Combustion



(d) Indicated mean effective pressure

**Fig. 2** Effects of ammonia ratios on the combustion characteristics of the ADDC engine

179 **Fig. 2** shows the effects of ammonia ratios on the combustion characteristics of the ADDC engine.  
180 As shown in the **Fig. 2a** and **Fig. 2b**, the peak cylinder pressure and peak HRR of the ADDC engine  
181 gradually decrease as the ammonia ratio increases because of the slow combustion velocity and low  
182 combustion temperature of ammonia. Although the premixed ammonia in the engine inlet can form  
183 a homogeneous fuel-air mixture in the intake stroke, the ammonia can only be ignited by the diesel  
184 and cannot self-ignite in the ADDC engine. Therefore, the primary exothermic process of the ADDC  
185 mode is mainly determined by the combustion velocity of the diesel injected into the cylinder. The  
186 increase in the ammonia ratio is accompanied by a decrease in the diesel ratio, so that the combustion  
187 rate of engine slows down, resulting in a gradual decrease in the peak cylinder pressure and peak  
188 HRR as the ammonia ratio increases. This indicates that a high proportion of ammonia premixing  
189 can lead to deterioration in combustion under the conditions of low equivalence ratios, and therefore  
190 a larger proportion of pilot fuel or other combustion strategies are required to enhance combustion  
191 and thus overcome the combustion inertia of ammonia in such conditions.

192 As can be seen in **Fig. 2c**, the change in ammonia ratio mainly affects the CD and has no  
193 significant effect on the ID. This illustrates that the ID of the ADDC mode is primarily determined  
194 by the diesel with high CN, while the combustion process is influenced by the combined effect of  
195 ammonia and diesel. Among them, when the ammonia ratio is below 40%, due to the high amount  
196 of diesel-air mixture formed before the combustion, the higher combustion temperature of the initial  
197 combustion stage facilitates the subsequent diffusion combustion process and thus leads to an  
198 overall shorter CD. However, the CD increases rapidly when the ammonia ratio is further increased,

199 reaching a CD of more than 20°CA at an 80% ammonia ratio. On the one hand, the reduced diesel  
200 ratio makes it difficult to form sufficient premixed gases and results in low initial combustion  
201 temperature. On the other hand, the low flame temperature of the ammonia further inhibits the  
202 combustion process. Finally, it can be seen from **Fig. 2d** that the IMEP of the engine decreases  
203 continuously as the ammonia ratio increases. The CA50 almost keeps constant at most ammonia  
204 ratios, except at the ammonia ratios of 70% and 80%, where there is a significant delay due to the  
205 low diesel injection mass. Combined with the HRR curves, it can be observed that the main reason  
206 for the decrease in IMEP with the increase in the ammonia ratio is the decrease in total cyclic heat  
207 release due to the lower combustion efficiency. Accordingly, it can be concluded that restoring the  
208 work capacity of the ammonia-fueled engine is primarily a solution for overcoming the combustion  
209 inertia and quenching effects of ammonia, thereby improving the overall combustion efficiency.

### 210 *3.2 Effects of ammonia ratios on the flame development of the ADDC engine*

211 To further explore the combustion process of the ADDC mode in-depth, this section provides  
212 further analysis of the flame development history and flame characteristics using the high-speed  
213 photography. The flame images during the main combustion period are selected for comparative  
214 analysis.



**Fig. 3** Flame development history of the ADDC mode at different ammonia ratios

215 **Fig. 3** shows the flame development history of the ADDC mode at different ammonia ratios. It  
 216 can be observed that a large area of high-brightness yellow-white flame appears in the region  
 217 covered by the diesel spray during the pure diesel combustion (PDC) mode. The large area of high-  
 218 brightness yellow-white flame disappears after the introduction of ammonia, and only a small high-

219 brightness yellow-white flame appears in the central area of the cylinder. The appearance of the  
220 high-brightness yellow-white flame is due to the formation of the fuel-rich region in the diesel spray  
221 region, which shows obvious diffusion combustion, and the carbon soot generation as well as the  
222 combustion temperature during diffusion combustion is higher, thus forming an obvious high-  
223 brightness flame. In addition, the small amount of high-brightness yellow-white flame in the  
224 cylinder center is due to diffusion combustion caused by insufficient injection pressure when the  
225 solenoid valve of diesel injector is seated. As the proportion of ammonia increases, the in-cylinder  
226 flame gradually changes from a yellow-white flame to a relatively low-brightness orange flame. The  
227 reason is that different from the combustion luminescence of carbon-based fuel which is mainly  
228 caused by the high-temperature carbon soot radiation, the luminescence of ammonia combustion  
229 comes mainly stems the radiation produced by intermediate products of ammonia combustion such  
230  $\text{NO}_2$  and  $\text{NH}_2$ .

231 It can also be seen from **Fig. 3** that the flame generally starts at the end of the diesel spray and  
232 then gradually spreads along the diesel spray to the cylinder center in the ADDC mode. Furthermore,  
233 due to the relatively low equivalence ratio used in this study (the equivalence ratios of PDC mode  
234 and 80% ammonia ADDC mode are 0.241 and 0.235, respectively), it can be seen that the ammonia  
235 flame is mainly concentrated around the diesel flame and the flame propagation distance is short.  
236 This is mainly due to the fact that ammonia has a relatively inert and quench-prone combustion,  
237 which is further exacerbated by the strong in-cylinder flow of CI engines which is used to enhance  
238 the mixing of the diesel spray. In addition, the combustion process of the ADDC mode is more  
239 concentrated when the ammonia ratio is low. Among them, a large ammonia burning flame occurs  
240 during  $2^\circ\text{CA ATDC} - 4^\circ\text{CA ATDC}$  at a 20% ammonia ratio, while the flame that appears after  $5^\circ\text{CA}$

241 ATDC is mainly due to the evaporative burning of the diesel attached to the cylinder wall. As the  
 242 ammonia ratio increases, the duration of the main combustion process is prolonged, which shows  
 243 an obvious ammonia combustion flame at  $2^{\circ}\text{CA ATDC}$  -  $7^{\circ}\text{CA ATDC}$  under the condition of an 80%  
 244 ammonia ratio. This may be due to the fact that although a large amount of diesel can increase the  
 245 combustion temperature when the ammonia ratio is low, the ammonia flame is more easily quenched  
 246 due to the relatively low ammonia equivalence ratio. When the ammonia ratio is higher, although  
 247 the energy introduced into the cylinder by diesel is lower, the stability of ammonia combustion  
 248 enhances due to the increase in the ammonia equivalence ratio. Furthermore, since the flame in the  
 249 ADDC mode is concentrated in the region covered by the diesel spray, the injection strategy and  
 250 injector structure parameters can be adjusted so that the diesel spray covers a larger volume of the  
 251 combustion chamber and thus increases the combustion efficiency.

252 To quantify the influence of the ammonia ratio on the flame behavior of the ADDC engine, the  
 253 flame center movement curves during combustion, the image hue and saturation of the brightest  
 254 moments of the flame were further extracted, as shown in **Fig. 4** and **Fig. 5** respectively, while the  
 255 FR percentage and FNL of the combustion process were extracted, as shown in **Fig. 6**.

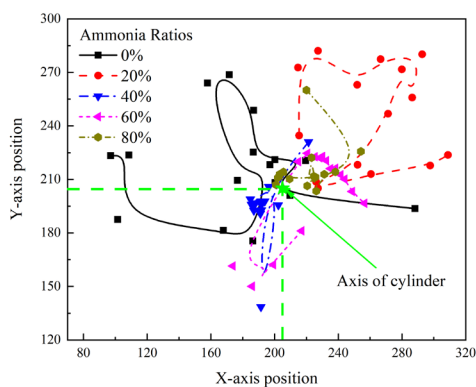


**Fig. 4** The flame center movement curves of

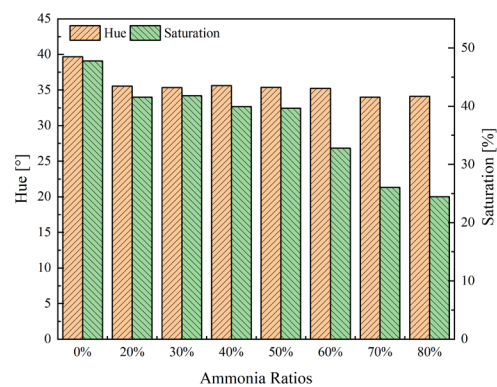


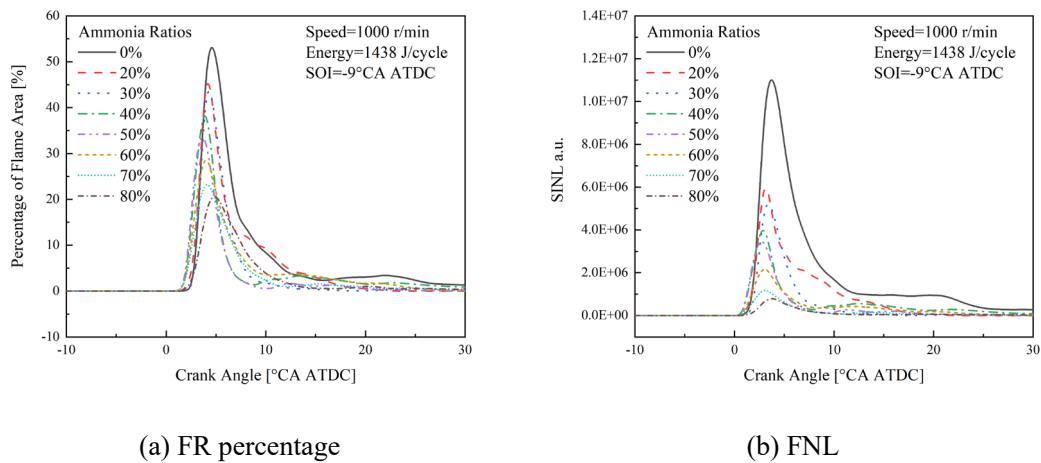
**Fig. 5** The hue and saturation of combustion

the ADDC mode at different ammonia ratios                      images of the ADDC mode at different  
ammonia ratios

256        As can be seen in **Fig. 4**, the movement of the flame center during the combustion process is  
257        evident when the ammonia ratio is low, and the flame center gradually stabilizes around the cylinder  
258        axis as the ammonia ratio increases. This is because the diffusion combustion is more obvious when  
259        the ammonia ratio is lower, and the in-cylinder airflow movement during diffusion combustion has  
260        a greater impact on the fuel volatilization and the combustion process, so the center position of the  
261        flame changes more significantly. At the same time, the flame center is shifted considerably in the  
262        later stage of combustion due to the volatilization of the wet wall fuel caused by the large injection  
263        mass of diesel. It is evident that the flame center moves within a wide range at the condition of pure  
264        diesel and 20% ammonia ratio. When the ammonia ratio is high, a more homogeneous ammonia/air  
265        mixture is formed in the cylinder, while the combustion velocity and flame propagation speed of  
266        ammonia are slow, and the effect of in-cylinder airflow movement on the flame distribution of  
267        ammonia combustion is reduced.

268        From **Fig. 5**, it can be seen that the flame hue of the PDC mode is 39.7, and the flame color tends  
269        to be yellow, while the ADDC mode appears as an orange flame with a hue of around 35. The flame  
270        hue of the ADDC mode almost keeps constant at the different ammonia ratios, which also indicates  
271        that the ammonia flame is wrapped around the outside of the diesel flame in the ADDC mode, and  
272        that the images captured by high-speed photography are the ammonia flame on the outside. In  
273        addition, it can be demonstrated that the hue of ammonia flame does not vary significantly with the  
274        equivalence ratio under the test conditions and that the flame hue cannot represent the intensity of  
275        ammonia combustion. Furthermore, it can also be seen that the flame saturation of the PDC mode

276 is 47.8, while the saturation gradually decreases with the addition of ammonia. It is worth noting  
 277 that the flame saturation does not change much when the ammonia ratio is in the range of 20%-50%,  
 278 while it decreases rapidly as the ammonia ratio increases in the range of 60%-80%. This may be  
 279 related to the difference in in-cylinder temperature caused by the change in HRR at the initial stage  
 280 of combustion.



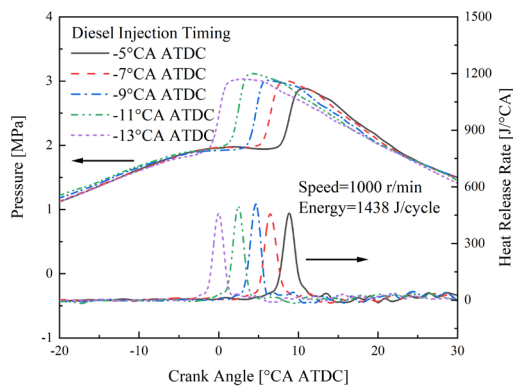
281 **Fig. 6** Effect of ammonia ratios on FR percentage and FNL of the ADDC mode

282 The FR shows the distribution of the flame in the combustion chamber, while the FNL  
 283 characterizes the intensity of the combustion to some extent, but the FNL is influenced by localized  
 284 regions of high brightness. As can be seen from **Fig. 6**, there is a difference in the effect of the  
 285 ammonia ratio on the FR and FNL. The peak of the FR percentage decreases as the ammonia ratio  
 286 increases, but the FR percentage curves are wider simultaneously. It means that although the diesel  
 287 ignition amount is relatively reduced with the increase in ammonia ratio, the duration of ammonia  
 288 combustion increases and the combustion efficiency of ammonia does not decrease significantly in  
 289 this way. In addition, the ammonia ratio has a greater effect on the FNL, compared to the effect on  
 290 the FR percentage, with the FNL decreasing rapidly as the ammonia ratio increases. The peak of FR  
 291 percentage and FNL of the 80% ammonia ratio ADDC mode decrease by 60% and 92%, respectively,

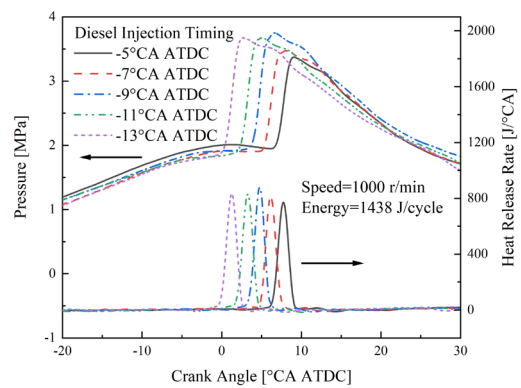
292 compared to the peaks at PDC mode. This is partly due to the reduction in the FR percentage, and  
 293 the main reason is that the flame from the bright carbon soot luminescence caused by diesel  
 294 combustion transforms into the radical radiation luminescence of ammonia combustion, and the  
 295 brightness of the ammonia flame radiation luminescence is much less than that of the carbon soot  
 296 luminescence.

### 297 3.3 Effects of DIT on the combustion characteristics of the ADDC engine

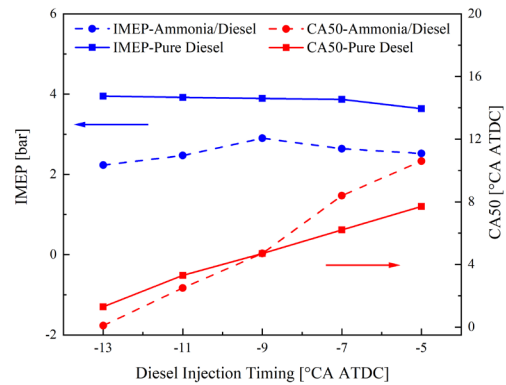
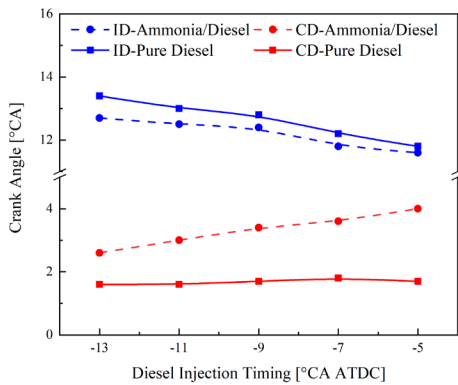
298 For the ADDC engine, the DIT directly determines the ignition timing and the subsequent  
 299 combustion process. This section provides further insight into the effect of DIT on the combustion  
 300 and flame development of the ADDC engine. The potential to improve the combustion process of  
 301 the ADDC engine by adjusting the DIT is explored.



(a) ADDC mode



(b) PDC mode



302 **Fig. 7** Effect of DIT on combustion characteristics of the ADDC mode and PDC mode

303 **Fig. 7** shows the effect of DIT on combustion characteristics of the ADDC mode and PDC mode.

304 Since the ammonia introduced into the intake burns slowly and quenches easily, compared to the

305 PDC mode, the ADDC mode has the lower peak cylinder pressure and peak HRR at different DITs.

306 And the peak cylinder pressure and peak HRR for both the two combustion modes do not change

307 significantly as the DIT advances. As the ignition timing of the ADDC mode depends principally

308 on the DIT, it can be seen from **Fig. 7c** that the IDs of both the two combustion modes are slightly

309 prolonged with the advancement of the DIT but the overall change are not significant. As a result,

310 the ignition timing advances with the advanced DIT, and the combustion phases corresponding to

311 the peak cylinder pressure and peak HRR also advance. Moreover, it can also be seen from **Fig. 7c**

312 that the effects of DIT on CDs is different for the two combustion modes. The CD of the PDC mode

313 hardly varies with the DIT, whereas the CD of the ADDC mode shortens with the advance of the

314 DIT. The reason is that the introduction of ammonia slows down the combustion of diesel and this

315 effect is strongly influenced by the in-cylinder temperature and pressure. As the combustion process

316 gradually approaches the TDC with the advanced DIT, the higher temperature and pressure near the

317 TDC lead to a faster combustion rate and a shorter CD.

318 As can be observed in **Fig. 7d**, the CA50s in both combustion modes are advanced and close the

319 TDC with the advancement of DIT, but the IMEPs of the two combustion modes show different

320 trends. In the PDC mode, the IMEP increases slightly as the DIT advances due to the CA50 being

321 close to the TDC and thus the increased timeliness of combustion. In the ADDC mode, the IMEP

322 tends to increase and then decrease as the DIT advances. The highest IMEP is reached at the DIT of

323 -9° CA ATDC. Combined with the HRR curves in Fig. 7a, it can be seen that although the HRR  
 324 curves for the ADDC mode at different DITs all show a single-peaked trend, the HRR of the initial  
 325 combustion stage slows down as the DIT advances. As a result, the long CD caused by the delayed  
 326 injection facilitates the ignition of the ammonia, while the total heat release decreases as the DIT is  
 327 advanced, thus contributing to the decrease in IMEP. In combination with the effect of CA50  
 328 changes on IMEP, the IMEP of the ADDC mode shows a trend of increasing and then decreasing.  
 329 3.4 Effects of DIT on the flame development of the ADDC mode

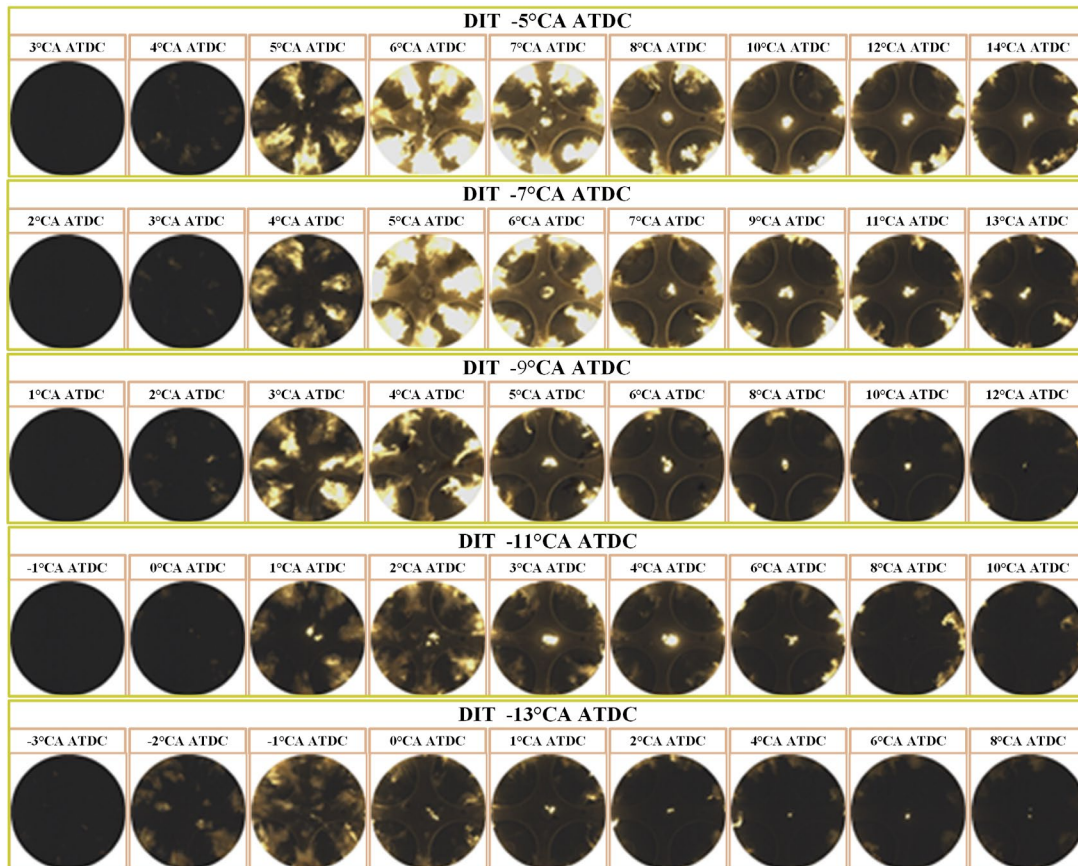
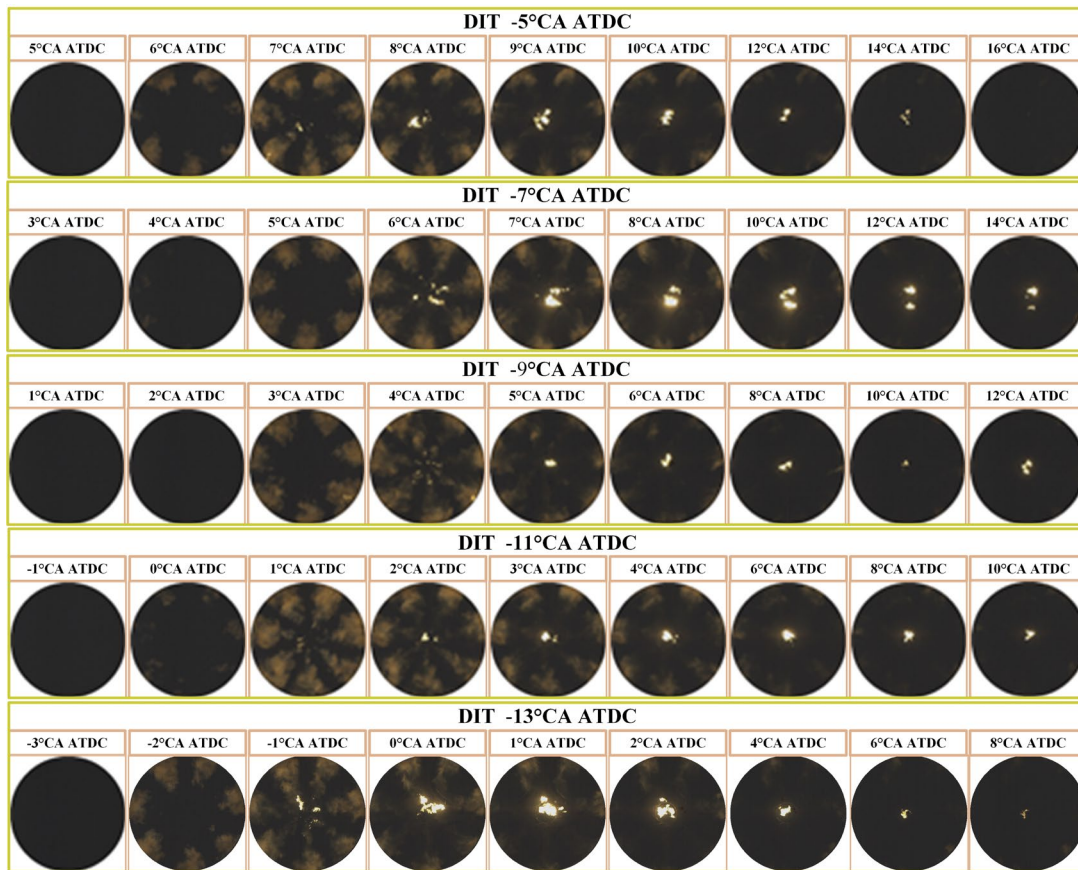


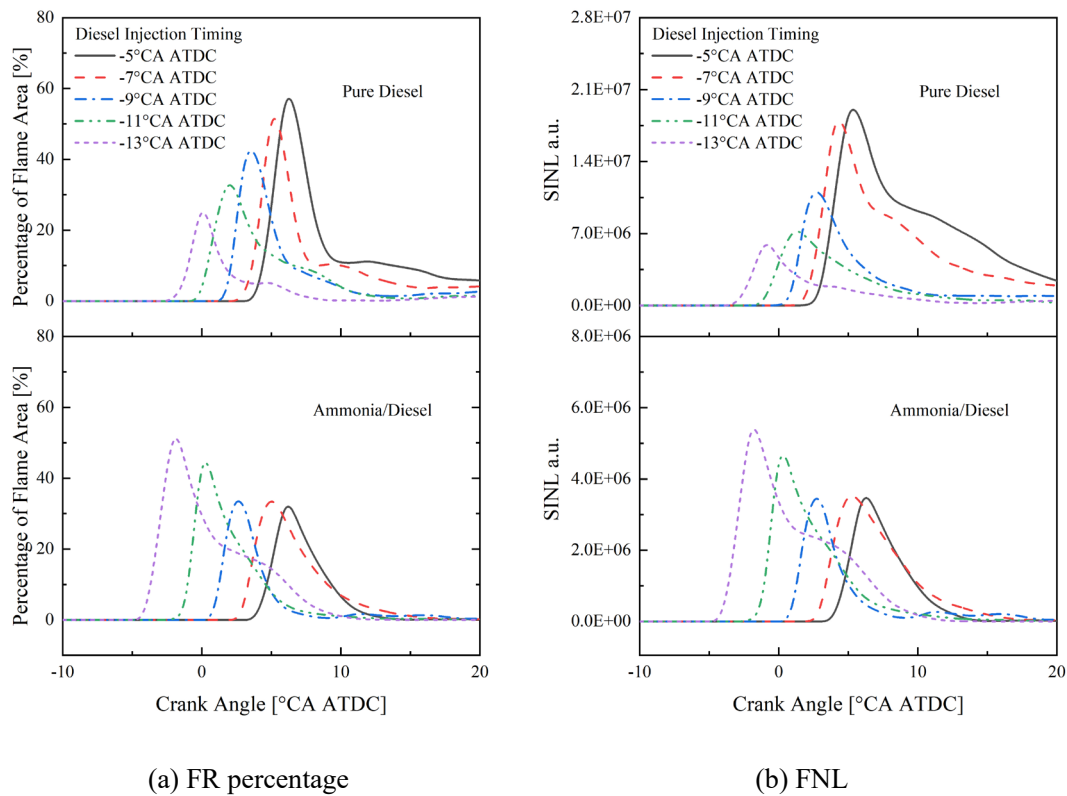
Fig. 8 Flame development history of the PDC mode at different DITs



**Fig. 9** Flame development history of the ADDC mode at different DITs

330 **Fig. 8** and **Fig. 9** show the flame development history of the PDC mode and ADDC mode at  
331 different DITs, respectively. As can be seen in **Fig. 8**, the flame luminescence in the PDC mode  
332 consists mainly of high-brightness yellow-white carbon soot luminescence, and the FR and FNL  
333 decrease significantly with the advance of DIT. Combined with the thermodynamic data, it can be  
334 seen that the ID is shorter when the DIT is postponed, the fuel cannot be adequately mixed and the  
335 tendency for diffusion combustion is more obvious, resulting in distinct carbon soot luminescence.  
336 When the DIT is advanced, there is sufficient time for the diesel to be mixed and thus a more  
337 uniformly distributed mixture is formed, so that the increase in premixing combustion ratio results  
338 in less high-brightness luminescence from carbon soot. As can be noticed in **Fig. 9**, unlike the  
339 yellow-white flame in the PDC mode, the flame in the ADDC mode is mainly the orange ammonia

340 flame. In addition, different from the PDC mode where the FR and FNL vary considerably with the  
 341 DIT, the ADDC mode maintains high FRs and FNLs at different DITs. This is because the ammonia  
 342 in the ADDC mode forms a more homogeneous fuel-air mixture during the intake stroke, and the  
 343 smaller diesel injection mass in this mode makes it easier to form a homogeneous mixture during  
 344 the ID. So, the DIT has an insignificant effect on the flame pattern of the ADDC mode.



345 **Fig. 10** Effect of DIT on FR percentage and FNL of the PDC mode and ADDC mode

346 **Fig. 10** shows the effect of DIT on FR percentage and FNL of the PDC mode and ADDC mode.  
 347 From **Fig. 10**, it can be seen that the FR and FNL for the two combustion modes show exactly  
 348 opposite trends with the DIT. The FR and FNL of the PDC mode decrease rapidly with the  
 349 advancement of the DIT due to the reduction of the diffusion combustion percentage. The peak of  
 350 FR percentage and FNL of the PDC mode at the DIT of  $-13^{\circ}\text{CA ATDC}$  decrease by 32.4% and  
 351  $1.36\text{E}7$ , respectively, compared to the peaks at DIT of  $-5^{\circ}\text{CA ATDC}$ . However, for the ADDC mode,

352 the FR and FNL increase instead as the DIT advances, but the change is smaller compared to that in  
353 the PDC mode. The peak of FR percentage and FNL of the ADDC mode at the DIT of  $-13^{\circ}\text{CA}$   
354 ATDC increase by 22.3% and  $2.25\text{E}6$ , respectively, compared to the peaks at the DIT of  $-5^{\circ}\text{CA}$   
355 ATDC. Among them, the increased FR and FNL may be due to the combustion process is close to  
356 the TDC, where the high temperature and pressure condition favors the radioluminescence of the  
357 carbon soot as well as the intermediate products of ammonia combustion. The small variation in the  
358 FR and FNL at different DITs indicates that the diesel with high reactivity still has a good ignition  
359 performance when the DIT is postponed.

360 Combined with **Fig. 7d**, it can be noticed that although the advanced DIT optimizes combustion  
361 timeliness, the IMEP decreases instead at the ADDC mode. This is probably due to the fact that  
362 when the diesel is injected in advance, the CD is shorter, which is not conducive to the ignition of  
363 ammonia, while when the DIT is postponed, the in-cylinder temperature and pressure are lower, and  
364 the slower combustion of diesel promotes the ignition of more ammonia. This indicates that different  
365 from the PDC mode where more premixed combustion needs to be organized to increase the  
366 combustion timeliness of engine, more diesel diffusion combustion needs to be organized to  
367 promote the combustion of ammonia and thus obtain a higher indicated power in the ADDC mode.  
368 At the condition of low equivalence ratios in the ADDC mode, it is possible to delay the injection  
369 of diesel to promote the combustion of ammonia but it is necessary to ensure that the combustion  
370 gravity is not delayed excessively.

#### 371 **4. Conclusions**

372 In this study, an optical diagnostic of the ADDC mode is conducted using a self-built optical  
373 engine. The flame development and combustion process of the ADDC mode are analyzed in-depth

374 using high-speed photography and combustion analysis methods. The combustion enhancement  
375 method and control strategy of the ammonia-fueled engine are proposed. The key findings can be  
376 obtained as follows:

377 (1) The ignition timing of the ADDC mode is mainly determined by the DIT, while the  
378 combustion process is influenced by both the premixed ammonia and the diesel injected into the  
379 cylinder. The combustion inertia and low flame temperature of ammonia lead to a decrease in the  
380 peak cylinder pressure and peak HRR with an increasing ammonia ratio, while the CA50 is severely  
381 delayed when the ammonia ratio is too high. Compared to the PDC mode, ammonia premixing leads  
382 to lower cyclic heat release and therefore lower engine IMEP.

383 (2) In contrast to the yellow-white flame produced by the radiation of high-temperature carbon  
384 soot in the PDC mode, the orange flame in the ADDC mode is mainly derived from the radiation  
385 produced by intermediate products of the ammonia combustion process such as  $\text{NO}_2$  and  $\text{NH}_2$ . The  
386 peak of FR percentage and FNL of the 80% ammonia ratio ADDC mode decrease by 60% and 92%,  
387 respectively, compared to the peaks at PDC mode. The ammonia flame of the ADDC mode is mainly  
388 concentrated around the diesel flame, which has a short flame propagation distance. The ADDC  
389 mode achieves good ignition performance at different ammonia ratios.

390 (3) Different from the PDC mode in which the CD is almost independent of the DIT, the ADDC  
391 mode has a significantly longer CD and a gradually delayed CA50 as the DIT is postponed.  
392 Combining the effects of the heat release and CA50, the IMEP of the PDC mode increases slightly  
393 as the DIT advances, while the IMEP of the ADDC mode shows a tendency to increase and then  
394 decrease.

395 (4) The effects of the DIT on the FR and FNL in the PDC mode and the ADDC mode show the

396 opposite trends. The FR and FNL in the PDC mode decrease rapidly with the advance of the DIT,  
397 and the flame pattern in the ADDC mode does not respond significantly to the DIT. The distinct  
398 ammonia combustion flame can be observed in the ADDC mode at all the DITs. Compared to the  
399 PDC mode, the ADDC mode requires an appropriate postponement of the DIT to organize more  
400 diffusive combustion of the diesel, and thus to promote the ammonia combustion for higher  
401 indicated thermal efficiency.

402

### 403 **Notes**

404 The authors declare no competing financial interest.

### 405 **Acknowledgments**

406 This work was supported by the National Natural Science Foundation of China (Project code:  
407 52202470); Natural Science Foundation of Jilin Province (Project code: 20220101205JC,  
408 20220101212JC); Free Exploration Project of Changsha Automotive Innovation Research Institute  
409 of Jilin University (Project code: CAIRIZT20220202); Horizon 2020 MSCA (Project code: H2020-  
410 MSCA-RISE- 778104-ThermaSMART).

### 411 **References**

- 412 [1] Liu A, Chen Y, Cheng X. Social cost of carbon under a carbon-neutral pathway. *Environmental*  
413 *Research Letters* 2022;17(5):054031. <https://doi.org/10.1088/1748-9326/ac6819>
- 414 [2] Kabir E, Kumar P, Kumar S, Adelodun AA, Kim K-H. Solar energy: Potential and future  
415 prospects. *Renewable and Sustainable Energy Reviews* 2018;82:894-900.  
416 <https://doi.org/10.1016/j.rser.2017.09.094>

- 417 [3] Rohrig K, Berkhout V, Callies D, Durstewitz M, Faulstich S, Hahn B, et al. Powering the 21st  
418 century by wind energy—Options, facts, figures. *Applied Physics Reviews* 2019;6(3):031303.  
419 <https://doi.org/10.1063/1.5089877>
- 420 [4] Paredes MG, Padilla-Rivera A, Güereca LP. Life Cycle Assessment of Ocean Energy  
421 Technologies: A Systematic Review. *Journal of Marine Science and Engineering* 2019;7(9):322.  
422 <https://doi.org/10.3390/jmse7090322>
- 423 [5] Hänggi S, Elbert P, Bütler T, Cabalzar U, Teske S, Bach C, et al. A review of synthetic fuels for  
424 passenger vehicles. *Energy Reports* 2019;5:555-569. <https://doi.org/10.1016/j.egy.2019.04.007>
- 425 [6] Koochi-Fayegh S, Rosen MA. A review of energy storage types, applications and recent  
426 developments. *Journal of Energy Storage* 2020;27:101047.  
427 <https://doi.org/10.1016/j.est.2019.101047>
- 428 [7] Banu A, Bicer Y. Review on CO<sub>x</sub>-free hydrogen from methane cracking: Catalysts, solar energy  
429 integration and applications. *Energy Conversion and Management: X* 2021;12:100117.  
430 <https://doi.org/10.1016/j.ecmx.2021.100117>
- 431 [8] Kobayashi H, Hayakawa A, Somarathne KDKunkuma A, Okafor Ekenechukwu C. Science and  
432 technology of ammonia combustion. *Proceedings of the Combustion Institute* 2019;37(1):109-133.  
433 <https://doi.org/10.1016/j.proci.2018.09.029>
- 434 [9] Liu H, Ampah JD, Zhao Y, Sun X, Xu L, Jiang X, et al. A Perspective on the Overarching Role  
435 of Hydrogen, Ammonia, and Methanol Carbon-Neutral Fuels towards Net Zero Emission in the  
436 Next Three Decades. *Energies*. 16. 2023. <https://doi.org/10.3390/en16010280>
- 437 [10] Manoharan Y, Hosseini SE, Butler B, Alzhahrani H, Senior BT, Ashuri T, et al. Hydrogen Fuel  
438 Cell Vehicles; Current Status and Future Prospect. *Applied Sciences* 2019;9(11):2296.

- 439 <https://doi.org/10.3390/app9112296>
- 440 [11] Chakraborty S, Dash SK, Elavarasan RM, Kaur A, Elangovan D, Meraj ST, et al. Hydrogen  
441 Energy as Future of Sustainable Mobility. *Frontiers in Energy Research* 2022;10:893475.  
442 <https://doi.org/10.3389/fenrg.2022.893475>
- 443 [12] Yue M, Lambert H, Pahon E, Roche R, Jemei S, Hissel D. Hydrogen energy systems: A critical  
444 review of technologies, applications, trends and challenges. *Renewable and Sustainable Energy  
445 Reviews* 2021;146:111180. <https://doi.org/10.1016/j.rser.2021.111180>
- 446 [13] MacFarlane DR, Cherepanov PV, Choi J, Suryanto BHR, Hodgetts RY, Bakker JM, et al. A  
447 Roadmap to the Ammonia Economy. *Joule* 2020;4(6):1186-1205.  
448 <https://doi.org/10.1016/j.joule.2020.04.004>
- 449 [14] Valera-Medina A, Xiao H, Owen-Jones M, David WIF, Bowen PJ. Ammonia for power.  
450 *Progress in Energy and Combustion Science* 2018;69:63-102.  
451 <https://doi.org/10.1016/j.peccs.2018.07.001>
- 452 [15] Valera-Medina A, Amer-Hatem F, Azad AK, Dedoussi IC, de Joannon M, Fernandes RX, et al.  
453 Review on Ammonia as a Potential Fuel: From Synthesis to Economics. *Energy & Fuels*  
454 2021;35(9):6964-7029. <https://doi.org/10.1021/acs.energyfuels.0c03685>
- 455 [16] Berwal P, Kumar S, Khandelwal B. A comprehensive review on synthesis, chemical kinetics,  
456 and practical application of ammonia as future fuel for combustion. *Journal of the Energy Institute*  
457 2021;99:273-298. <https://doi.org/10.1016/j.joei.2021.10.001>
- 458 [17] Chehade G, Dincer I. Progress in green ammonia production as potential carbon-free fuel. *Fuel*  
459 2021;299:120845. <https://doi.org/10.1016/j.fuel.2021.120845>
- 460 [18] Yapicioglu A, Dincer I. A review on clean ammonia as a potential fuel for power generators.

461 Renewable and Sustainable Energy Reviews 2019;103:96-108.  
462 <https://doi.org/10.1016/j.rser.2018.12.023>

463 [19] Xing H, Stuart C, Spence S, Chen H. Alternative fuel options for low carbon maritime  
464 transportation: Pathways to 2050. Journal of Cleaner Production 2021;297:126651.  
465 <https://doi.org/10.1016/j.jclepro.2021.126651>

466 [20] Cardoso JS, Silva V, Rocha RC, Hall MJ, Costa M, Eusébio D. Ammonia as an energy vector:  
467 Current and future prospects for low-carbon fuel applications in internal combustion engines.  
468 Journal of Cleaner Production 2021;296:126562. <https://doi.org/10.1016/j.jclepro.2021.126562>

469 [21] Li J, Lai S, Chen D, Wu R, Kobayashi N, Deng L, et al. A Review on Combustion  
470 Characteristics of Ammonia as a Carbon-Free Fuel. Frontiers in Energy Research 2021;9:760656.  
471 <https://doi.org/10.3389/fenrg.2021.760356>

472 [22] Chai WS, Bao Y, Jin P, Tang G, Zhou L. A review on ammonia, ammonia-hydrogen and  
473 ammonia-methane fuels. Renewable and Sustainable Energy Reviews 2021;147:111254.  
474 <https://doi.org/10.1016/j.rser.2021.111254>

475 [23] Kurien C, Mittal M. Review on the production and utilization of green ammonia as an alternate  
476 fuel in dual-fuel compression ignition engines. Energy Conversion and Management  
477 2022;251:114990. <https://doi.org/10.1016/j.enconman.2021.114990>

478 [24] Chiong M-C, Chong CT, Ng J-H, Mashruk S, Chong WWF, Samiran NA, et al. Advancements  
479 of combustion technologies in the ammonia-fuelled engines. Energy Conversion and Management  
480 2021;244:114460. <https://doi.org/10.1016/j.enconman.2021.114460>

481 [25] Dimitriou P, Javaid R. A review of ammonia as a compression ignition engine fuel. International  
482 Journal of Hydrogen Energy 2020;45(11):7098-7118.

483 <https://doi.org/10.1016/j.ijhydene.2019.12.209>

484 [26] Li T, Zhou X, Wang N, Wang X, Chen R, Li S, et al. A comparison between low- and high-  
485 pressure injection dual-fuel modes of diesel-pilot-ignition ammonia combustion engines. Journal of  
486 the Energy Institute 2022;102:362-373. <https://doi.org/10.1016/j.joei.2022.04.009>

487 [27] Boretti A. Novel dual fuel diesel-ammonia combustion system in advanced TDI engines.  
488 International Journal of Hydrogen Energy 2017;42(10):7071-7076.  
489 <https://doi.org/10.1016/j.ijhydene.2016.11.208>

490 [28] Tornatore C, Marchitto L, Sabia P, De Joannon M. Ammonia as Green Fuel in Internal  
491 Combustion Engines: State-of-the-Art and Future Perspectives. Frontiers in Mechanical  
492 Engineering 2022;8:944201. <https://doi.org/10.3389/fmech.2022.944201>

493 [29] Nadimi E, Przybyła G, Emberson D, Løvås T, Ziółkowski Ł, Adamczyk W. Effects of using  
494 ammonia as a primary fuel on engine performance and emissions in an ammonia/biodiesel dual-fuel  
495 CI engine. International Journal of Energy Research 2022;46(11):15347-15361.  
496 <https://doi.org/10.1002/er.8235>

497 [30] Reiter AJ, Kong S-C. Combustion and emissions characteristics of compression-ignition engine  
498 using dual ammonia-diesel fuel. Fuel 2011;90(1):87-97. <https://doi.org/10.1016/j.fuel.2010.07.055>

499 [31] Niki Y, Nitta Y, Sekiguchi H, Hirata K. Diesel Fuel Multiple Injection Effects on Emission  
500 Characteristics of Diesel Engine Mixed Ammonia Gas Into Intake Air. Journal of Engineering for  
501 Gas Turbines and Power 2019;141(6). <https://doi.org/10.1115/1.4042507>

502 [32] Sun X, Li M, Li J, Duan X, Wang C, Luo W, et al. Nitrogen Oxides and Ammonia Removal  
503 Analysis Based on Three-Dimensional Ammonia-Diesel Dual Fuel Engine Coupled with One-  
504 Dimensional SCR Model. Energies. 16. 2023. <https://doi.org/10.3390/en16020908>

- 505 [33] Pastor JV, Olmeda P, Martín J, Lewiski F. Methodology for Optical Engine Characterization by  
506 Means of the Combination of Experimental and Modeling Techniques. *Applied Sciences* 2018;8  
507 (12):2571. <https://doi.org/10.3390/app8122571>
- 508 [34] Cui Y, Liu H, Wen M, Feng L, Ming Z, Zheng Z, et al. Optical diagnostics of misfire in partially  
509 premixed combustion under low load conditions. *Fuel* 2022;329:125432.  
510 <https://doi.org/10.1016/j.fuel.2022.125432>
- 511 [35] Lee C-f, Pang Y, Wu H, Hernández JJ, Zhang S, Liu F. The optical investigation of hydrogen  
512 enrichment effects on combustion and soot emission characteristics of CNG/diesel dual-fuel engine.  
513 *Fuel* 2020;280:118639. <https://doi.org/10.1016/j.fuel.2020.118639>
- 514 [36] Peterson B, Baum E, Dreizler A, Böhm B. An experimental study of the detailed flame transport  
515 in a SI engine using simultaneous dual-plane OH-LIF and stereoscopic PIV. *Combustion and Flame*  
516 2019;202:16-32. <https://doi.org/10.1016/j.combustflame.2018.12.024>
- 517 [37] Cui Y, Liu H, Wen M, Feng L, Wang C, Ming Z, et al. Optical diagnostics and chemical kinetic  
518 analysis on the dual-fuel combustion of methanol and high reactivity fuels. *Fuel* 2022;312:122949.  
519 <https://doi.org/10.1016/j.fuel.2021.122949>
- 520 [38] Marchitto L, Tornatore C. Optical techniques applied to internal combustion engines for soot  
521 detection – a review. *2022 IEEE International Workshop on Metrology for Automotive* 2022:145-  
522 149. <https://doi.org/10.1109/MetroAutomotive54295.2022.9855025>
- 523 [39] Soid SN, Zainal ZA. Spray and combustion characterization for internal combustion engines  
524 using optical measuring techniques – A review. *Energy* 2011;36(2):724-741.  
525 <https://doi.org/10.1016/j.energy.2010.11.022>
- 526 [40] Zhang H, Sun W, Guo L, Yan Y, Sun Y, Zeng W, et al. Optical diagnostic study of coal-to-

527 liquid/butanol blend and dual-fuel combustion of a CI engine. Fuel 2022;320:123978.  
528 <https://doi.org/10.1016/j.fuel.2022.123978>

529 [41] Zhang R, Chen L, Wei H, Li J, Chen R, Pan J. Understanding the difference in combustion and  
530 flame propagation characteristics between ammonia and methane using an optical SI engine. Fuel  
531 2022;324:124794. <https://doi.org/10.1016/j.fuel.2022.124794>

532 [42] Ihracska B, Korakianitis T, Ruiz P, Emberson DR, Crookes RJ, Diez A, et al. Assessment of  
533 elliptic flame front propagation characteristics of iso-octane, gasoline, M85 and E85 in an optical  
534 engine. Combustion and Flame 2014;161(3):696-710.  
535 <https://doi.org/10.1016/j.combustflame.2013.07.020>

536 [43] Hult J, Matamis A, Baudoin E, Mayer S, Richter M. Spatiotemporal flame mapping in a large-  
537 bore marine diesel engine using multiple high-speed cameras. International Journal of Engine  
538 Research 2019;21(4):622-631. <https://doi.org/10.1177/1468087419853429>

539 [44] Lee S, Yoon S, Kwon H, Lee J, Park S. Effects of engine operating conditions on flame  
540 propagation processes in a compression ignition optical engine. Applied Energy 2019;254:113642.  
541 <https://doi.org/10.1016/j.apenergy.2019.113642>

542 [45] Di Iorio S, Magno A, Mancaruso E, Vaglieco BM. Analysis of the effects of diesel/methane  
543 dual fuel combustion on nitrogen oxides and particle formation through optical investigation in a  
544 real engine. Fuel Processing Technology 2017;159:200-210.  
545 <https://doi.org/10.1016/j.fuproc.2017.01.009>

546 [46] Zhang R, Chen L, Wei H, Li J, Ding Y, Chen R, et al. Experimental investigation on reactivity-  
547 controlled compression ignition (RCCI) combustion characteristic of n-heptane/ammonia based on  
548 an optical engine. International Journal of Engine Research 2022:14680874221124452.

549 <https://doi.org/10.1177/14680874221124452>